

# **DEVELOPMENT OF TRANSVERSE JOINTS FOR FULL-DEPTH PRECAST DECK PANELS INCORPORATING RIBBED-SURFACE GFRP BARS, HPC AND UHPFRC**

**Mahmoud Sayed-Ahmed**, Ph.D. Candidate, Civil Engineering Department, Ryerson University,  
Toronto, Canada

**Khaled Sennah**, Ph.D., P.E., PCI Member, Civil Engineering Department, Ryerson University,  
Toronto, Canada

## **ABSTRACT**

Corrosion of reinforcing steel in bridge decks decreases life expectancy of bridge superstructures, leading to costly and frequent maintenance or replacement. The use of glass fiber reinforced polymer (GFRP) bars as internal reinforcement is a viable option for the replacement of deteriorated concrete bridge deck slabs due to steel bar corrosion. The proposed research investigates the use of ribbed-surface GFRP bars in cast-in-place bridge deck slabs as well as precast bridge deck slab of prefabricated full-depth deck panels to accelerate bridge construction. In this research, three joints between precast panels were developed using straight GFRP bars embedded in a closure strip filled with ultra-high performance fiber reinforced concrete (UHPFRC). High-performance concrete of 70-MPa compressive strength was used to cast the prefabricated panels. Two control cast-in-place slabs reinforced with steel bars and GFRP bars, respectively, were cast to form the baseline of the structural performance of the developed jointed panels. Concentric and eccentric wheel loading were applied at the joint to expose it to pure bending and combined bending and shear, respectively. The results show that precast slab with zigzag-shaped closure strip performed similarly to the steel-reinforced and GFRP-reinforced cast-in-place slabs with respect to ultimate flexural strength. The jointed slab with eccentric loading showed a slight increase in ultimate wheel load resistance compared to identical precast slab with concentric loading case. In addition, the failure mode was flexural in case of precast slabs with concentric loading over the joint, compared to combined flexural and shear failure mode in case of precast slabs with eccentric loading at the joint.

**Keywords:** GFRP-bars, Bridge deck slabs, Prefabricated girders, Closure strips, Ultra-high Performance Fiber Reinforced Concrete, Full Depth-Precast Deck Panel.

## INTRODUCTION

One of the prefabricated bridge system used to accelerate bridge construction is the full-depth, full width, precast concrete deck slab with transverse joint placed over steel or concrete girders. In this system shown in Fig. 1, grout pockets are provided to accommodate clusters of shear connectors welded to steel girders or embedded in concrete girders. Literature survey revealed that PCI Report along with other ABC manuals produced by US DOTs specify the use of high-performance concrete (HPC) with 70 to 100 MPa compressive strength in precast deck panels to provide sufficient strength and durability. With the use of UHPFRC and GFRP bars in the closure strip, the performance of the transverse panel-to-panel joints in bridge system shown in Fig. 1 needs to be investigated at ultimate and fatigue limit states.

Recent surveys of the state of practice of full-depth, full-width panel-girder system and joints were conducted elsewhere (among them: NCHRP<sup>1</sup> Badie and Tadros<sup>2</sup>; Hieber and Wacker<sup>3</sup>). Connections suitable for simple and continuous spans for composite design were developed using different means including headed reinforcing steel bars, steel couplers and post-tensioning the precast panels. Although deck panel post-tensioning puts the joint in compression and secure it against leakage, it increases the cost of the deck system and delays deck construction. A few authors (among them: Graybeal<sup>4</sup>; Li et al.<sup>5</sup>) have dealt with panel-to-panel longitudinal joints in bulb-tee girders. While others authors have (among them: Graybeal<sup>6</sup>; Issa et al.<sup>7</sup>) dealt with panel-to-panel transverse joints, all using steel reinforcing bars. None of these transverse joints were tested using GFRP bars. Zhu et al.<sup>8</sup> proposed continuous transverse U-bar joint details, incorporating projecting reinforced steel bars from the jointed panels which can provide negative moment continuity in multi-span bridges, however no pretensioning was used. Based on ultimate and fatigue test results, the developed transverse U-bar joint detail appeared to provide continuity of the reinforcement in the deck panels to carry tensile forces while acting compositely with the girders.

## NEW CONNECTION DETAILS

The prefabricated bridge system shown in Fig. 1 incorporates precast concrete panels placed side-by-side to form the bridge deck. In this system, the concrete deck slab is cast in a controlled environment at the fabrication facility and then transported to the construction site. One of the main issues inherent in these prefabricated systems is the presence of cold joints created by the closure pours and their potential impact on the overall deck system behavior. In addition, it is important to develop effective connection details between the prefabricated elements to provide continuity of reinforcement in the closure strips so that load sharing between girders is not compromised. Shah et al.<sup>9</sup> and Khalafalla and Sennah<sup>10</sup> developed deck joints having closure strip widths ranging from 125 to 425 mm with projecting steel bars and GFRP bars with headed ends, respectively.

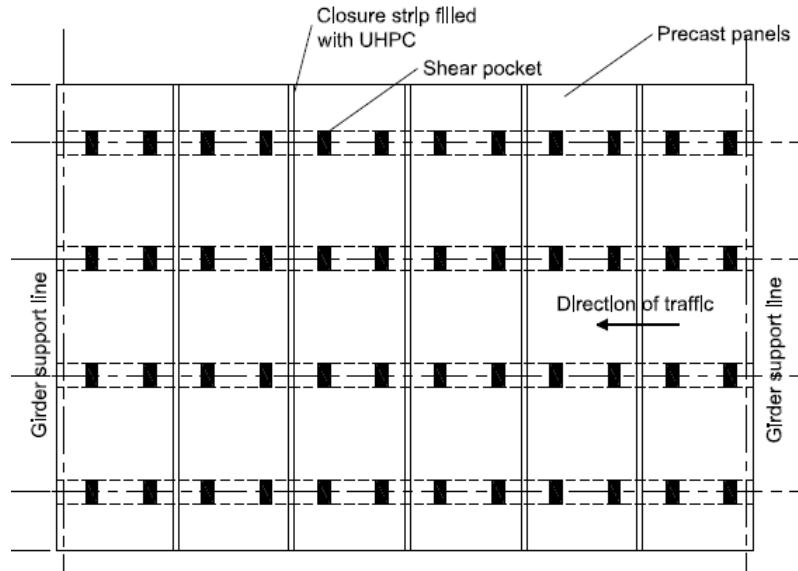


Fig. 1 Plan view of slab-on-girder bridge with full depth, full-width deck panels



Fig. 2 Views of GFRP bars

This paper introduces glass fibre reinforced polymer (GFRP) bars as main reinforcement in the precast panels, projecting in the closure strip with straight ends. FRPs, as non-corrodible materials, are considered as excellent alternative to reinforcing steel bars in bridge decks to overcome steel corrosion-related problems. Since it is less expensive than carbon and aramid FRPs, Glass FRP (GFRP) bars are more attractive for bridge deck applications. The GFRP bars used in this study have a tensile strength of 1188 MPa, compared to 400 MPa yield strength of reinforcing steel bars. It should be noted that the specified modulus of elasticity of the steel bars and GFRP bars are 200 and 64 GPa, respectively. The special “ribbed” surface profile of these bars, shown in Fig. 2, ensure optimal bond between the concrete and the bar. The favorable FRP characteristics include (i) high-strength-to-weight ratio; (ii) resistant to corrosion; (iii) freeze and thaw resistance; and (iv) high chemical resistant<sup>11</sup>.

Three details for the joints between precast panels were proposed incorporating GFRP bars as depicted in Figure 3. The first proposed joint has a 200 mm wide closure strip as shown in Fig. 3-a. In this joint, both the top and bottom GFRP bars in the precast slab project into the joint with a 175-mm anchorage length. It is assumed that temporary form work will be used to close the bottom of the closure strip to hold UHPFRC materials before hardening. In bridge construction, Ontario Ministry of Transportation (MTO) adopts the standard 225 mm thick cast-in-place deck slab in Ontario bridges. This slab thickness incorporates 65 mm top concrete cover as recommended by CHBDC<sup>12</sup> for reinforcing steel bars for protection against possible corrosion. However, with the use of non-corrosive FRP bars, the deck concrete cover can be reduced to 40 mm as specified in CHBDC with the use of FRP reinforcement. This change the FRP-reinforced deck slab thickness 200 mm, thus reducing the material of the deck slab by about 12%. As a result, it is decided to conduct this research using 200 mm thickness for all slabs considered in this study. A vertical shear key, shown in Fig. 3-a, was used on each side of the joint to allow for shear resistance between the jointed parts. As mentioned earlier, the common practice in Canada for precast concrete bridge decks is to use concrete with compressive strength of 35MPa. However, given the trend in US DOTs of using high-performance concrete (HPC), it was



avoid material spilling. The third proposed joint has a 100-mm wide closure strip with staggered 100 mm wide trapezoidal-shaped (zigzagged-shaped) interlock between the precast flanges as shown in the plan of Fig. 3-c. In this connection, the top and bottom GFRP bars of the precast slab project into the joint with a 175 mm anchorage length. A temporary form work will be required to hold the cast UHPFRC into the closure strip before hardening.

It should be noted that this joint with zigzag shape and vertical shear key at joint edges would be a good choice for the closure strip at the negative moment region since it will provide continuity through bar splice along with interlocking of the zigzagged UHPFRC closure strip with the zigzagged edges of the precast panel. The use of 70 MPa concrete along with this joint in the vicinity of the piers would allow for enhanced continuity that increase moment resistance of the composite slab-girder section at ultimate and fatigue limit state designs.

## **EXPERIMENTAL PROGRAM**

The experimental program investigated two types of loading that can be applied at the closure strip region, namely concentric and eccentric truck wheel loading. Figure 4-a shows a schematic diagram of the jointed slab with truck wheel load located over the joint creating pure bending on UHPFRC. Figure 4-b shows the wheel load located at the edge of joint creating combined shear and bending in the UHPFRC. As such, the test setups considered in this study includes both (i) pure flexural tests, and (ii) combined flexural-shear tests.

The experimental program included six full-scale deck slab specimens 2500-mm long and 200-mm thick. A 600-mm slab width is considered for a slab strip. The 600-mm width is assumed oriented in the direction normal to the traffic, while the slab span is oriented in the direction of traffic. It should be noted that the selection of this slab size and details is considered for the sake of correlating test results for the jointed precast slab with identical cast-in-place slabs reinforced by either steel bars or GFRP bars to examine the transverse capacity of the joint under bending of combined bending and shear. In fact, the results from this research can be applied to the joint between bulb-tee girders since the objective of this testing is to qualify the jointed precast slab to be “as good as” the cast-in-place slab of similar geometry, concrete quality and reinforcement sizes but with different reinforcement material.

In this study, the wheel load will be distributed only over a 600 mm width of the slab and over a length of 250 mm in the direction of slab span. The span of the slab was taken as 2000 mm with a slab total length of 2500 mm to accommodate proper bars anchorage beyond the supporting points. The first deck slab specimen, S1, is formed of cast-in-place concrete reinforced using steel bars. In this research, 3-20M reinforcing steel bars spaced at 200 mm on center were used as bottom and top layers representing the CHBDC-specified minimum steel reinforcement of 1.0% of the concrete area. Transverse 10M steel bars were used at the top and bottom layers at 300 mm spacing. Figure 5-a shows view of the steel reinforcement in slab S. The second deck slab strip, S2, is similar to cast-in-place slab S1 but with 3-20M straight GFRP bars spaced at 200 mm on center, as bottom tension reinforcement. Transverse reinforcement consists of 20M GFRP bars were used at the top and bottom layers at 300 mm on center spacing. Figure 5-b shows view of the GFRP reinforcement in slab S2.

The third deck slab, S3, is similar to slab S2 but uses the precast deck joint shown in Fig. 3-a. The amount and spacing of GFRP bars in the precast flanges were the same as those for the cast-in-place deck slab S2. Figure 5-b shows a view of the GFRP bar layout in S3 slab formwork, while Fig. 6-a shows a view of straight GFRP bars projecting into the closure strip of slab S3 before casting the UHPFRC. It should be noted that slabs S1 to S3 were loaded with the wheel load located concentrically over the joint as depicted in Fig. 4-a. The fourth deck slab, S4, is identical to the joined precast slab S3, and had the joint eccentrically loaded as depicted in Figure 4-b.

The fifth slab S5 incorporates the trapezoidal-shaped (zigzagged-shaped) interlocking closure strip between precast panels shown in Fig. 3-c. The slab size and GFRP reinforcement in S5 is identical to those for slabs S3 and S4. Figure 5-c shows a view of the GFRP bar layout in S5 slab formwork, while Figure 6-b shows a view of the straight GFRP bars projecting into the closure strip of slab S5 before casting the UHPFRC. The sixth deck slab, S6, is similar to the joined precast slabs S3 and S4 but with the closure strip details shown in Fig. 3-b. Figure 5-d shows view of the GFRP bar layout in S6 slab formwork, while Figure 6-c shows view of the straight GFRP bars projecting into the closure strip of slab S6 before casting the UHPFRC. Table 1 summarizes the main variables of the tested slabs. The straight GFRP bars used in specimens S2, S3, S4, S5 and S6 were of ribbed-surface, as shown in Fig. 2, with 1188-MPa tensile strength and 60-GPa modulus of elasticity.



a) Slab S1



b) Slab S2 and S3



c) Slab S5



d) Slab S6

Fig. 5 Reinforcement layout in slab specimens



a) Closure strip for S3 and S4



b) Closure strip for slab S5



c) Closure strip for S6

Fig. 6 Plan views of closure strip in jointed slabs

Concrete having a specified 28-day compressive strength of 70 MPa was used for both cast-in-place and precast deck slabs. Standard cylinders of 150-mm diameter and 300-mm height were cast concurrently with the casting of the deck slabs. An average of three cylinders were cast and stored close to the test samples to ensure the same curing conditions after casting. The tested cylinder had a concrete compressive strength of 76.94 MPa. Ultra-High-Performance Fiber Reinforced Concrete (UHPFRC) of compressive concrete strength of 140 MPa was used for closure strip. During the pouring of the UHPFRC into the precast deck slab closure strips, standard cylinders of 100-mm diameter and 200-mm height were cast and kept close to the test samples. Table 1 summarizes the average strength of cylinders tested on the day of slab testing.

The structural response during the static loading of the specimens was captured through the use of electronic instrumentation. Potentiometers and Linear variable differential transducers (LVDTs) were used to measure deflections at mid-span of the slab specimens. A static patch load, simulating CHBDC truck wheel load was applied to examine the structural behavior and ultimate load carrying capacity of the proposed connection details as compared to the control cast-in-place slabs S1 and S2 reinforced with steel and GFRP bars, respectively. Slabs S1, S2, and S3 were tested under a 250x600 mm single patch load at the center of their clear span.

Figures 7 and 8 show the locations of the wheel load at the mid-span for slabs S1 and S2, respectively. While Figure 9-a shows the wheel load applied concentrically over the joint. This patch load is equivalent to the foot print of CHBDC wheel load of 87.5 kN. The slab ends were simply-supported over roller support at one end and hinged support at the other end. Slabs S4, S5, and S6 were tested under a 250x600 mm single patch load located at the edge of the joint as shown in Figs. 10-a, 11-a and 12-a, respectively.

To conduct static load tests to-collapse, the jacking load was applied in increments to allow for visual inspection of the specimens and to mark cracks. The available data acquisition system was used to capture readings from sensors as well as the load cell located between the jacking piston and the top of the deck slab. After every load increment, start of tension cracks and crack propagations were monitored. It should be noted that the incremental loading technique was used during testing. The specimen was loaded to 10 kN, followed by load release. The specimen was loaded to 20 kN, followed by load release. These incremental loading steps were repeated with a total load increase of 10 kN in each step until the specimen failed. The following section discusses the structural behavior of the test specimens.

Table 1. Summary of slab configurations and test results

Slab	Bottom Reinforcement	Slab type	Wheel load location	$f'_c$ MPa		Ultimate load (kN)	Ultimate Deflection (mm)	Failure mode
				Concrete	UHPFRC			
S1	Steel straight bars (3-20M)	Cast-in-place	Concentric	76.94	-	169.47	29.81	Flexural
S2	GFRP straight bars (3-20M)	Cast-in-place	Concentric	76.94	-	161.34	42.24	Flexural
S3	GFRP straight bars (3-20M)	Precast with 200 mm closure strip filled with UHPFRC	Concentric	76.94	141.11	148.39	37.84	Flexural
S4	GFRP straight bars (3-20M)	Precast with 200 mm closure strip filled with UHPFRC	Eccentric	76.94	141.11	152.53	22.12	Flexural-shear
S5	GFRP straight bars (3-20M)	Precast with zigzag-shaped closure strip filled with UHPFRC	Eccentric	76.94	166.58	162.52	26.89	Flexural-shear
S6	GFRP straight bars (3-20M)	Precast with 200 mm closure strip and bottom projecting slab and filled with UHPFRC	Eccentric	76.94	141.11	111.33	24.26	Flexural



Fig. 7 Test setup and crack pattern at failure of slab S1

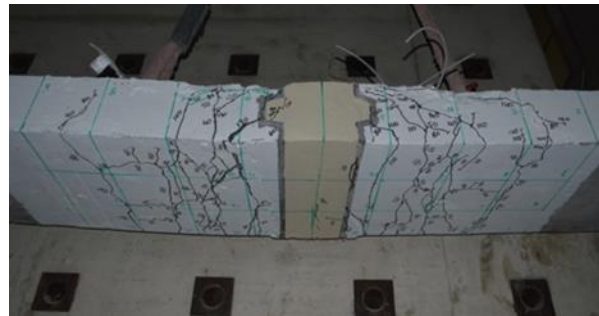


Fig. 8 Test setup and crack pattern at failure of slab S2



a) Test setup

b) Crack pattern at the joint region



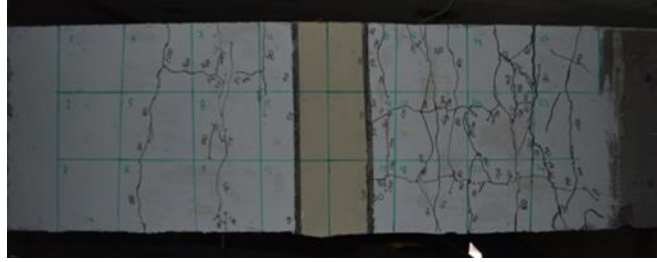
c) Crack pattern at the bottom and side of the slab

Fig. 9 Test setup and crack pattern at failure of slab S3



a) Test setup

b) Crack pattern at the joint region



c) Crack pattern at the bottom of the slab

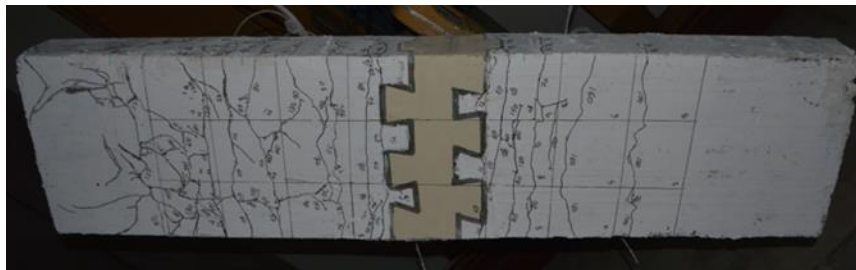
Fig. 10 Test setup and crack pattern at failure of slab S4



a) Test setup



b) Crack pattern at the joint region



c) Crack pattern at the bottom of the slab

Fig. 11 Test setup and crack pattern at failure of slab S5



a) Test setup



b) Crack pattern at the joint region



c) Close-up view of the joint



d) Flexural crack at bottom of the joint

Fig. 12 Test setup and crack pattern at failure of slab S6

## TEST RESULTS

This section discusses the structural behavior of the tested specimens in the form of crack pattern, slab deflection and ultimate load carrying capacity. Figure 7 shows the crack pattern at failure at the side of the slab for the cast-in-place slab S1 with steel reinforcing bars. It was observed that the first visual flexural crack appeared at the bottom of the slab at the mid-span location at a load of 28 kN. Other flexural cracks appeared at the quarter points of the span and propagated towards the top surface of the slab with each increase in load till failure. Crushing of concrete at the top surface of the slab at the mid-span location was observed at the maximum jacking load of 169.47 kN and slab deflection of 29.81 mm, leading to pure flexural flexure. Figure 8 shows the crack pattern at failure of cast-in-place slab S2 with GFRP bars. It was observed that the first visible flexural crack appeared at a load of 28 kN. Other flexural crack appeared at higher load increments and spread over a length greater than that for slab S1. The slab failed mainly due to large flexural cracks, with concrete crushing at the top surface of slab at an ultimate load of 161.34 kN and deflection of 42.24 mm. By comparing the ultimate load capacity of slabs S1 and S2, it can be observed that the GFRP-reinforced slab exhibited a flexural strength of about 4.8% less than that for a similar slab reinforced with steel bars and a deflection at failure of about 42% more than the steel-reinforced slab. This increase in deflection in the GFRP –reinforced barrier may be attributed to the significant reduction in the modulus of elasticity of the GFRP bars when compared with steel bars.

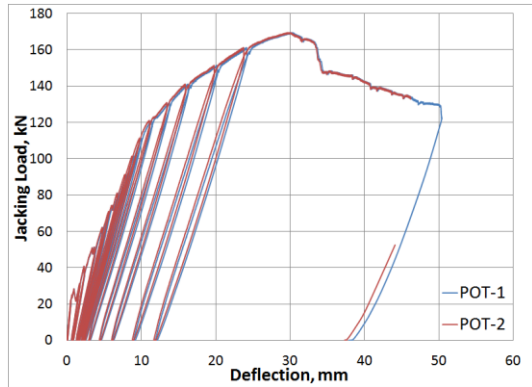
Figures 9-b and 9-c show the crack pattern at failure of precast slab S3 with 200-mm wide closure strip and projecting straight GFRP bars into the UHPFRC-filled closure strip. It was observed that the first hairline cracks were formed at the cold joint between the precast concrete and the closure strip. These fine cracks started to widen gradually with increase in applied load. Several flexural, as well as flexural-shear, cracks appeared in the precast slab closer to the closure strip, with a wide flexural crack at both sides of the cold joint. Failure of slab S3 was at an ultimate load of 148.39-kN and a deflection of 37.84-mm. By comparing the ultimate load capacity of slabs S2 and S3, it can be observed that the GFRP-reinforced jointed slab exhibited a flexural strength of about 8% less than that for a similar cast-in-place slab. This slight decrease in slab flexural strength should be considered acceptable given the presence of the joint at the maximum moment location with short splice length of GFRP bars. It should be noted that light

flexural crack appeared in the UHPFRC at the slab mid-span, with no visible cracks appeared in the UHPFRC material at the free sides of the slab as depicted in Figs. 9-b and 9-c.

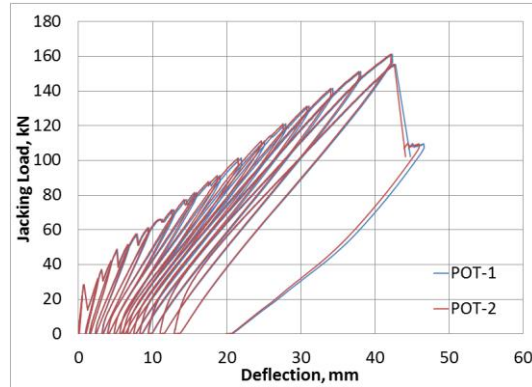
Figures 10-b and 10-c show the crack pattern at failure of the precast GFRP-reinforced slab S4 with eccentric truck wheel loading at the joint. It was noticed that the first hairline cracks were formed at the cold joint between the precast concrete and the closure strip at a load of 30 kN. These fine cracks started to widen gradually with an increase in applied load. Few flexural cracks appeared in the precast slab closer to the closure strip. Close to failure, a wide diagonal-shear crack, as depicted in Fig. 10-b, propagated along the slab between the support and the applied load location, leading to slab failure. Failure of slab S4 occurred at an ultimate load of 152.53-kN and a deflection of 22.12-mm. Comparing slabs S3 and S4, it can be observed that the slabs ultimate load increased slightly (i.e. by 3%) as a result of using eccentric loading rather than concentric loading at the closure strip, while the slab ultimate deflection decreased by about 41%. This may be attributed to the fact that the shear span of the precast slab with eccentric loading decreases, leading to a higher load carrying capacity.

Figure 11-b and 11-c shows the crack pattern at failure of precast slab S5 with the 100-mm wide closure strip and staggered 100-mm wide trapezoidal-shaped interlocking, and GFRP bars projected into the joint. It was noticed that the first hairline cracks were formed at the cold joint between the precast concrete and the closure strip at a load of 15 kN. These fine cracks started to widen gradually with an increase in applied load. A few flexural cracks appeared in the precast slab closer to the closure strip as shown in Fig. 11-c. Prior to failure, a wide diagonal flexural crack appeared on one both side of the cold joint at the quarter point of the precast slab as depicted in Fig. 11-b that led to failure. Failure of slab S5 occurred at an ultimate load of 162.52-kN and a deflection of 26.89-mm. No cracks appearing in UHPFRC at the bottom or the sides of the joint. As such, it can be concluded that slab S5 performed as well as the steel-reinforced slab S1 (i.e. 4% difference) and GFRP-reinforced slab (i.e. 0.7% difference) with respect to ultimate strength.

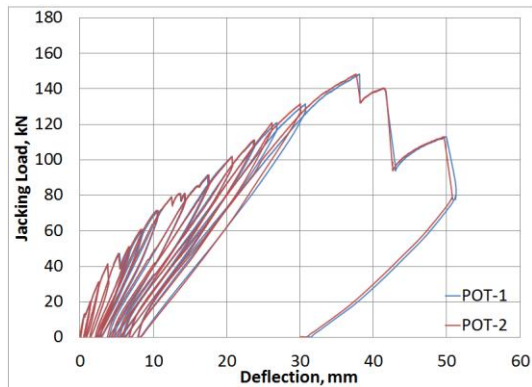
Figure 12-b through 12-d shows the crack pattern at failure of the precast slab S6 with 200-mm wide closure strip and projected bottom slab segment. It was observed that the first hairline cracks were formed at the cold joint between the precast concrete and the closure strip and propagated towards the top of the slab with load increase as depicted in the close-up in Fig. 12-c at a load of about 30 kN. These cracks widened with increase in the applied load as depicted in Fig. 12-d, leading to concrete crushing at the top surface of the slab. Other flexural cracks appeared between the joint and the quarter point of the precast slab as depicted in Fig. 12-b. The slab failed at an ultimate load of 111.33-kN and a deflection of 24.26-mm. It can be noted that slab S6 has a flexural capacity less than those for the steel-reinforced slab S1 and the GFRP-reinforced slab S2 by 34% and 31%, respectively.



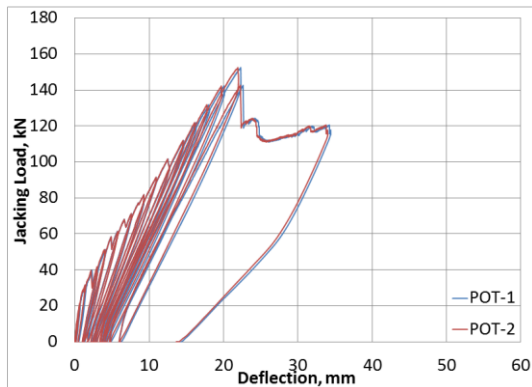
(a) Slab S1



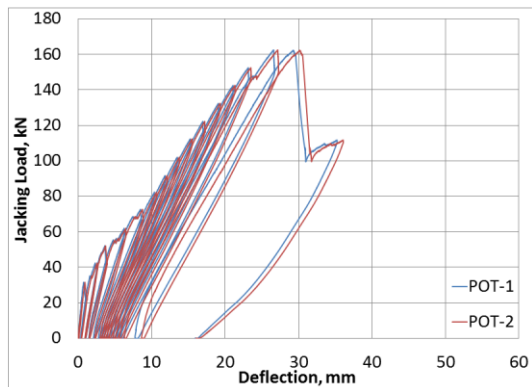
(b) Slab S2



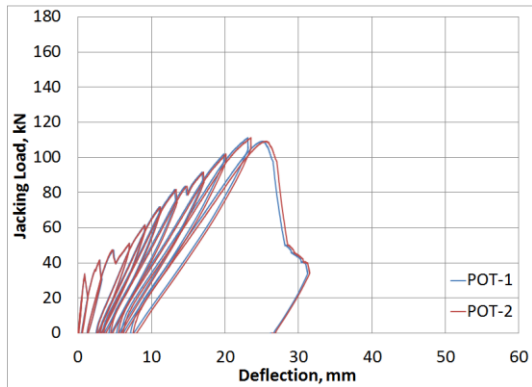
(c) Slab S3



(d) Slab S4



(e) Slab S5



(f) Slab S6

Fig. 13 Load-deflection relationships obtained under the loading-points of slab specimens

Figure 13 depicts the incremental load-deflection history of all tested specimens. Although the load-deflection history presents a measure of the change in slab flexural stiffness due to cracking, and yielding of steel in case of steel-reinforced slab, with increase in applied load, the given data can be used further to determine slab ductility under wheel load. Such analysis as well as forthcoming testing of these slabs under fatigue loading is expected to provide engineers with clear picture on the preferred joint between precast slabs for enhanced strength, fatigue service life and durability. Figure 14 depicts the combined load-deflection for the all tested specimens.

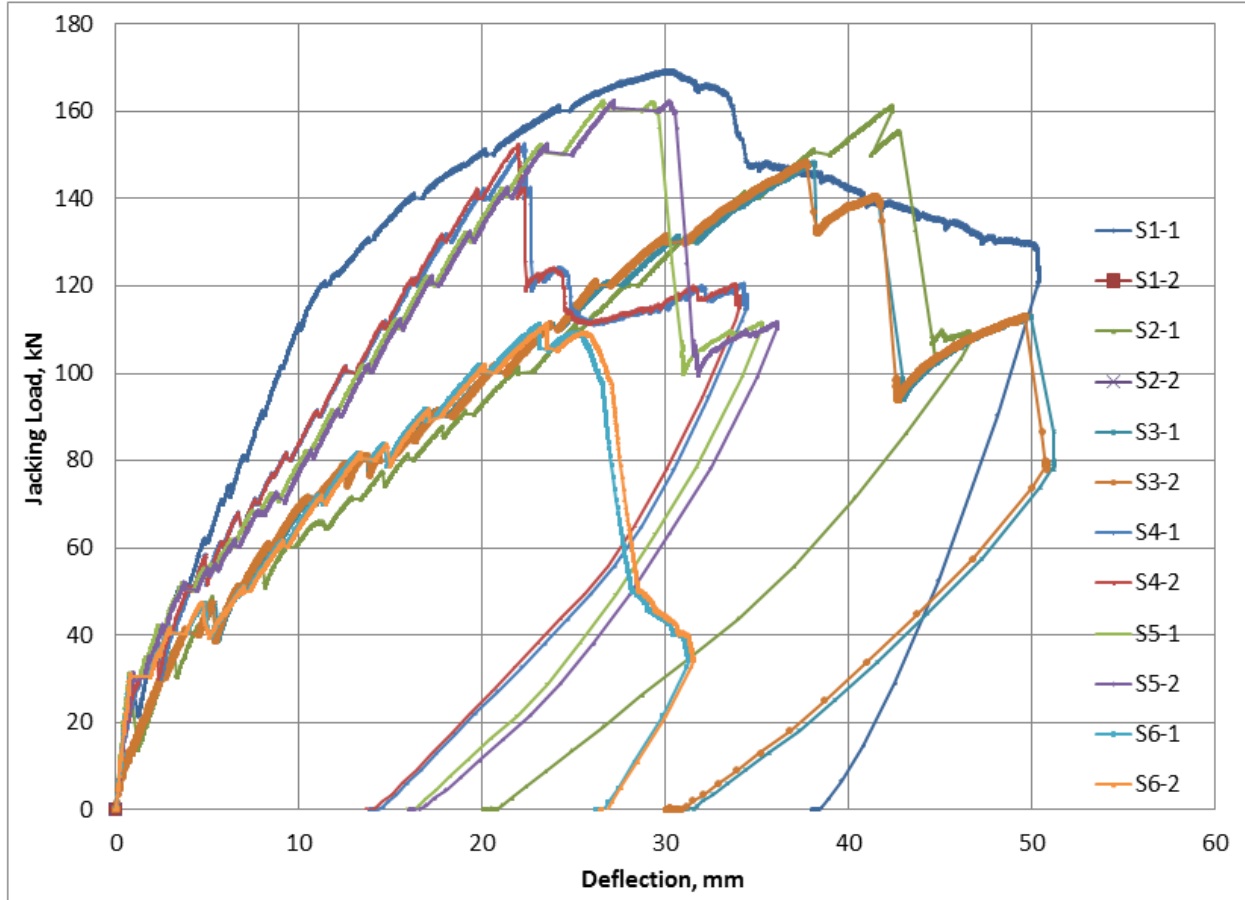


Fig. 14 Combined load-deflection curves for all specimens

## CONCLUSIONS

This paper investigates the use of GFRP bars in cast-in-place bridge deck slabs as well as in precast bridge deck slab for prefabricated bridge girders to determine their structural behavior and ultimate load carrying capacities when subjected to CHBDC wheel loading. The results were correlated to a control slab reinforced with steel bars. Based on the experimental results, it can be concluded that the ultimate load capacity of GFRP-reinforced cast-in-place slab is about 5% greater than the capacity of a similar slab reinforced with steel bars in accordance with the CHBDC and having the same cross-sectional area as the GFRP bars. Also, it can be observed that the GFRP-reinforced jointed slab with a 200 mm wide joint width with vertical shear keys exhibited a flexural strength about 8% less than that for a similar cast-in-place slab. Comparing jointed precast slabs with different applied load patterns, it was observed that the slab ultimate load slightly increased (i.e. by 3%) as a result of using eccentric loading rather than concentric loading at the closure strip, while the slab ultimate deflection decreased by about 41%. The precast slab with a zigzag-shaped joint appeared to be as good as the steel-reinforced slab (i.e. 4% difference) and GFRP-reinforced slab (i.e. 0.7% difference) with respect to ultimate strength. The precast slab with a 200-mm wide closure strip and projected bottom slab segment proved to have flexural capacity less than those for the steel-reinforced cast-in-place slab and the GFRP-reinforced cast-in-place slab 34% and 31%, respectively. Further tests are currently conducted to examine the fatigue life of the successful control joints under simulated vehicular wheel loading.

## ACKNOWLEDGMENTS

The authors would also like to acknowledge the support of Ontario Ministry of Transportation for funding this project, and Schoeck Canada Inc. for supplying the GFRP bars. Also, the authors would like to thank Lafarge North America Inc. for supplying the UHPFRC mix. Moreover, the authors would like to thank St. Marys / Canada Building Materials (CBM) for supplying the high-performance concrete.

## REFERENCES

- 1- NCHRP. 2011. Summary of Cast-In-Place Concrete Connections for Precast Deck Systems. Research Results Digest 355, Transportation Research Board, pp. 1-33.
- 2- Badie, S., and Tadros, M. 2008. NCHRP Report 584: Full-Depth Precast Concrete Bridge Deck Panel Systems. Transportation Research Board, Washington, D.C.
- 3- Hieber, D., and Wacker, J. 2005. State-of-the-Art Report on Precast Concrete Systems for Rapid Construction of Bridges. Report No. WA-RD 594.1, Washington State Department of Transportation, 112 pages.
- 4- Graybeal, B. 2010. Behavior of Field-Cast Ultra-High Performance Concrete Bridge Deck Connections Under Cyclic and Static Structural Loading. Federal Highway Administration, Report No. FHWA-HRT-11-023, 106 pp.
- 5- Li, L., Ma, Z., Griffey, M., Oesterle, R. 2011. Improved Longitudinal Joint Details in Decked Bulb Tees for Accelerated Bridge Construction: Concept Development, Journal of Bridge Engineering, 15(3): 327-336.
- 6- Graybeal, B.. 2006. Material Property Characterization of Ultra-High Performance Concrete,” Federal Highway Administration, Report No. FHWA-HRT-06-103, August 2006, 186 pp.
- 7- Issa, M., Salas, J., Shabila, H., and Alrousan, R. 2006. Composite Behavior of Precast Concrete Full-Depth Panels and Prestressed Girders. PCI Journal, 132-145.
- 8- Zhu, P., Ma, Z., Cao, Q., and French, C. 2012. Fatigue Evaluation of Transverse U-Bar Joint Details for Accelerated Bridge Construction. Journal of Bridge Engineering, 17:191-200.
- 9- Shah, K. Sennah, R. Kianoush, Siyin Tu and Clifford Lam. 2006. Flange-to-Flange Moment Connections for Precast Concrete Deck Bulb-Tee Bridge Girders. Journal of Prestressed Concrete Institute, PCI, 51(6): 86-107.
- 10- Khalafalla, I., and Sennah, K. 2013. Improved Longitudinal Joint Details in GFRP-reinforced Decked Bulb Tees for Accelerated Bridge Construction. Proceedings of PCI Convention and National Bridge Conference, Grapevine, Texas, p. 1-14.
- 11- [www.schoeck-canada.com](http://www.schoeck-canada.com).
- 12- CHBDC. 2006. Canadian Highway Bridge Design Code, CAN/CSA-S6-06. Canadian Standard Association, Toronto, Ontario, Canada.